Mathematical Biosciences and Engineering

https://www.aimspress.com/journal/mbe

MBE, 22(8): 2120–2151.
DOI: 10.3934/mbe.2025078
Received: 1 February 2025
Revised: 03 June 2025
Accepted: 12 June 2025
Published: 03 July 2025

Research article

Cooperation-conflict dynamics and ecological resilience under environmental disturbances

Suvranil Chowdhury, Sujit Halder, Kaushik Kayal and Joydev Chattopadhyay*

Agricultural and Ecological Research Unit, Indian Statistical Institute, Kolkata 700108, India

* **Correspondence:** Email: joydev@isical.ac.in.

Abstract: Ecosystem stability is increasingly threatened by rapid environmental fluctuations that alter species interactions and survival strategies. Traditional steady-state analyses often overlook transient dynamics that govern ecosystem responses to accelerating change. This study explored rate-induced tipping (R-tipping), a phenomenon where environmental change rates outpace species' adaptive capacity, triggering abrupt shifts between ecological states. Our findings demonstrate that species persistence depends on a delicate balance between cooperation-associated costs, population densities, and environmental variation rates. Under moderate fluctuations, species can track unstable states before reaching new equilibria, enhancing resilience. However, beyond critical thresholds, homoclinic and saddle-node bifurcations destabilize coexistence induced with increasing cooperation strength, leading to extinction cascades. By integrating time-dependent basin stability analysis, we uncovered mechanisms driving ecological transitions and identified key factors influencing long-term persistence. This research highlights the need for dynamic models to predict tipping events and informs conservation strategies for mitigating biodiversity loss in rapidly changing environments.

Keywords: transient states; alternative steady state; rate of environmental variation; tracking unstable states; ecosystem persistence; cost-associated cooperation; feed-forward mechanism

1. Introduction

Species have evolved adaptive strategies to survive and thrive amidst environmental fluctuations, shaping their interactions, habitat preferences, predation strategies, and grazing behaviors. Traditional models often focus on short-term, stationary variability using periodic or stochastic processes. However, recent research emphasizes long-term, directional changes through non-equilibrium frameworks, as steady-state analysis becomes inadequate for dynamic environments [1]. Long-term environmental changes, such as global climate shifts, can push species communities toward tipping points, raising questions about their adaptive capacity and ecosystem persistence. Despite evidence

that environmental changes impact prey-predator interactions through consumptive and non-consumptive pathways, key aspects of species dynamics and transient times to alternate states remain poorly understood. Gradual climatic shifts have historically enabled ecosystems to adapt through evolution and migration, while sudden events like volcanic eruptions or asteroid impacts triggered mass extinctions and collapses [2, 3]. In modern times, rapid human activities have accelerated environmental changes, evident in rising global temperatures, climate imbalances, habitat fragmentation, and frequent landslides [4–6]. These anthropogenic changes often exceed ecosystems' adaptive capacities, increasing tipping point occurrences. Ecosystem resilience, defined as the ability to absorb disturbances and reorganize while maintaining functions and structures, is crucial for ecosystem management [7, 8]. While steady-state mathematical models provide insights into resilience, they fall short of capturing the complexities of rapid environmental changes. Traditional models assume constant or slowly varying conditions, which fail to represent real-world dynamics. Therefore, dynamic approaches are essential to predict the impact of swift environmental changes and understand the non-linear interactions and feedback loops in ecological systems.

Climate change can disrupt plant nutrient balances, altering food quality and increasing toxicity [9, 10]. These changes affect herbivores' foraging behaviors and nutrient intake, often forcing them into less favorable habitats [11, 12]. Such habitat shifts can intensify competition due to overcrowding in new areas while reducing species density in old habitats, heightening extinction risks and disrupting population dynamics [13]. Understanding these complex dynamics under non-equilibrium conditions is essential for predicting ecosystem responses to continuous environmental change. As a response to adverse environmental scenarios, species may adopt various cooperative strategies to enhance defense mechanisms, improve predation efficiency, optimize resource use, and more. These strategies can significantly influence predation rates, dispersal patterns, competition dynamics, and foraging efficiency. However, in a broader sense, they ultimately contribute—directly or indirectly—to improving species fitness and overall growth rates. Despite these potential benefits, cooperative behaviors often incur associated costs. Thus, the balance between these costs and benefits serves as a key driver in shaping species interaction policies and persistence mechanisms [14].

Existing studies indicate that rising temperatures due to global warming can reduce an ecosystem's carrying capacity, elevate species' metabolic rates, and drive shifts toward over-exploitation or alternative food sources [15, 16]. Higher metabolic rates in warmer environments increase food demands for both prey and predators, leading to intensified foraging and predation pressure [17]. In response, prey may adopt herd behavior to improve foraging efficiency; however, this also raises cooperation costs by making them more detectable to predators [14, 18]. On the predator side, increased attack rates and energy demands may promote cooperative hunting. However, imbalanced protein-carbohydrate intake can reduce predation efficiency and disrupt coordinated hunting strategies [19]. As a result, the cost-benefit dynamics of cooperation become destabilized. Additionally, species that consume plants from highly toxic environments may experience disruptions in the gut-brain axis, impairing their anti-predator responses and alarm signaling [20]. Notably, both anti-predator movements and alarm signaling are cooperative traits with inherent costs [14, 18], which are likely to increase under changing environmental conditions.

Research on web spiders and grasshoppers highlights an intriguing cost-benefit trade-off, where rising temperatures prompted nursery web spiders to shift microhabitats, intensifying grasshopper

responses to predation risk [21, 22]. This heightened sensitivity to alarm signals and anti-predator movements enhances the cooperative benefits for prey species. Such findings suggest that beyond traditional predator-prey interaction parameters—such as predation pressure, numerical response, and the reproduction rate—environmental disturbances can significantly alter species' behavioral responses, influencing their cooperative or competitive strategies. Sentis et al. [23] further demonstrated that increased temperatures elevated biochemical production in beetle larvae, deterring conspecific females from oviposition and reducing the risk of egg predation. However, this protective mechanism inadvertently lowered fitness, making populations more vulnerable to extinction at low densities. Notably, these costs of cooperation escalate under fluctuating environmental conditions, particularly in species that adopt cooperative breeding strategies [24]. This suggests that environmental changes may regulate Allee thresholds and alter species' carrying capacities simultaneously. These strong biological insights underscore the need to investigate how environmental variability reshapes the cost-benefit balance of cooperation and its implications for population dynamics in globally changing ecosystems [25, 26]. However, no comprehensive modeling-based study has yet thoroughly captured these phenomena.

Thus, understanding how environment-driven variations in cooperation costs or benefits among prey species embodied overall population dynamics—especially when predator species also adapt their predation strategies to enhance survival—remains a central focus of this study. Through density-dependent reproduction rates, Chowdhury et al. [27] examined how varying cooperation intensity in prey species influences the cost-cooperation balance of the system, assuming there is no specialized predation response to prey cooperation (by employing Type I and Type II functional forms) in a constant environment. However, this assumption not only makes the dynamics more intriguing but also suggests that incorporating a more adaptive predation strategy could lead to a model formulation that better captures biologically relevant and ecologically rational phenomena. The concept of the "degree of partial cooperation", addressed by Chowdhury et al. [27], refers to the extent to which organisms engage in cooperative behaviors, including clustering or grouping, to improve their survival and fitness. This framework recognizes that cooperation may be less effective than traditionally assumed, either due to inherent costs or the influence of cognitive and selective cooperation strategies. To carry through the purpose of this study we choose to include the rate of the global environmental change-induced degree of partial cooperation in prey species.

Cost-associated cooperation [27] becomes particularly relevant in the context of global climate change, where accelerating environmental fluctuations are expected to induce drastic shifts in population densities [4, 5, 28]. Such shifts can often be attributed to the presence of multistability in system dynamics. In fact, under diverse ecological conditions, species may face extinction even before reaching a stable or oscillatory state. While Ramesh et al. [1] explored tipping events in metacommunity systems, the absence of both multistability and stable extinction equilibria leaves a crucial gap in understanding how transient times vary near such tipping points in single-patch systems. Chowdhury et al. [27] further demonstrated that in a predator-free system, increasing cooperation intensity initially benefits prey populations. However, as cooperation intensifies, predators may indirectly exploit cooperative behaviors to reestablish within the system, promoting coexistence—a result consistent with existing literature. Yet, beyond a critical threshold, the costs of cooperation surpass its benefits, ultimately pushing the species toward extinction directly from a stable oscillatory state. Investigating such complex ecological transitions further motivates our study,

where we analyze these dynamics through the "tracking unstable state" framework [1].

The journey of theoretical exploration of the characteristics of ecological communities either relies on deterministic setups or stochastic environments. In deterministic environments, steady-state analysis inherently assesses the basin stability—a measure of the likelihood that a system returns to its initial state after perturbation—as a traditional approach for observing the behavior of multistability [1, 29]. Basin stability plays a crucial role in understanding community dynamics, as it evaluates the ability of a system to withstand external disturbances. However, basin stability becomes a less effective technique if environmental changes consistently drive the system from one steady state to an alternate state that is not connected to the previous multistable configuration [30]. Such transitions may lead to the formation of entirely new community structures, potentially resulting in the loss of ecosystem services. Theoretical studies have incorporated periodic (e.g., seasonal) or stationary stochastic variations to model environmental changes. These approaches, while valuable, often mirror traditional models because they typically lead to community collapse through bifurcation-induced tipping (B-tipping) or noise-induced tipping (N-tipping) [31]. B-tipping occurs when slow parameter changes cause the system to reach a critical threshold, leading to a sudden transition, while N-tipping arises from random environmental fluctuations pushing the system over a tipping point.

In fact, when the predator extinction equilibrium or system-wide extinction equilibrium remains the only stable state over a specific parameter range, the trajectory of a time-varying environment inevitably converges to one of these extinction states. This scenario places species coexistence and survival in an ambiguous position. From an ecological perspective, such uncertainty in species survival probability necessitates identifying mechanisms that can significantly enhance species persistence. In this study, we address this challenge by incorporating environmental variation at a constant rate across multiple phenomena simultaneously—an aspect that, although acknowledged by ecologists, remains largely unexplored for single-patch systems in previous studies [1]. Furthermore, we demonstrate how environmental variation-driven multi-parameter changes reshape species' extinction probabilities, revealing critical insights into ecological resilience under dynamic environmental conditions. This approach introduces a novel perspective, making the study more comprehensive.

The paper is structured as follows: Section 2 introduces the model and explains the influence of environmental factors on prey growth and predator consumption rates. Section 3 explores the dynamics and existence of various steady states. In Section 4, global sensitivity analysis is conducted to account for parameter uncertainty in our model. Section 5 presents detailed observations under different environmental changes. Section 6 delves into the impact of environmental variations on bi-parameter analysis. Finally, the concluding section provides a comprehensive discussion and suggests future research directions.

2. Mathematical modeling approach

The construction of deterministic models to investigate biological phenomena requires a balance between simplicity, clarity, and accuracy. Hence, rather than solely aiding in the exploration of environmental change-driven impacts on the cost-benefit balance of cooperation, incorporating the "degree of partial cooperation" under environmental variation significantly enhances our understanding of how global environmental changes simultaneously influence multiple biological

phenomena in a more simplified way. Chowdhury et al. [27] suggested that beyond capturing the cost-cooperation conflict in species dynamics, the cost-associated cooperation modeling approach effectively represents complex phenomena such as strong demographic Allee effects and dynamic carrying capacity. More importantly, the thresholds of these traits vary with changes in the degree of cost-associated cooperation. Existing studies, as discussed earlier, indicate that environmental variation can have a significant influence on Allee thresholds, carrying capacity, and the cooperative nature of predation rates. However, tracking changes across multiple parameters—if not all—within a time-varying environment not only increases the complexity of the study but also poses challenges in effectively representing the dynamical results. Incorporating environmental variation in the intensity of cost-associated cooperation inherently induces variability in Allee effects and carrying capacity. Thus, selecting an appropriate two-parameter variation—such as cooperation intensity alongside competition or the predation rate—can provide a more simplified yet lucid representation of this complex multi-variable scenario.

Our approach to selecting a functional response term differs from that of Chowdhury et al. [27] for two primary reasons. First, the earlier study on cost-associated cooperation [27] employed type-I or type-II functional responses, primarily to avoid mathematical complexities. Second, their structural sensitivity analysis demonstrated that the dynamics under type-I functional responses remain structurally robust when extended to type-II, Ivlev, or tan-hyperbolic functional responses. However, their work did not provide biological justification for these choices. When prey species engage in cooperative behaviors like herding or clustering, predators often adjust their foraging tactics to enhance hunting efficiency. Rather than searching alone, predators tend to form coordinated groups that come together when prey is detected. This aggregation behavior increases the encounter rate between predators and prey, improving the success of predation compared to individual hunting efforts. This collective approach leads to a higher encounter rate compared to solitary hunting [32]. Such behaviors are observed in species like tuna, which forage in groups and aggregate when prey schools are detected [33]. Furthermore, in large prey groups, individual predators may not consume all available prey at once, allowing for continued predation over time. Cosner et al. [32] suggested a specific functional form to model such biology accurately, which was

$$g(x, y) = \frac{\rho xy}{1 + h\rho xy}. \tag{2.1}$$

This type of functional response (2.1) captures these dynamics by examining how predation rates are influenced by both the density of prey and the size of predator groups. However, the effectiveness of this strategy is influenced by several factors, including the communication range among predators and the prey's ability to disperse. These ecological factors make this functional response particularly useful in understanding systems where predators hunt cooperatively and adapt to changes in response to the cooperative behaviors of the prey. Here x and y represent prey and predator densities, respectively, and details for the rest of the parameters are given in Table 1. Thus, now our basic model in a constant environment will be structured as:

$$\begin{aligned} \frac{dx}{dt} &= rx^{\nu} - ax^2 - dx - \frac{\rho xy^2}{1 + h\rho xy}, \\ \frac{dy}{dt} &= \frac{c\rho xy^2}{1 + h\rho xy} - my. \end{aligned} \tag{2.2}$$

As suggested by Hamilton's Rule, cooperation occurs when the benefit-cost ratio exceeds 1, which is captured by the "degree of partial cooperation" in our model, providing biological justification for choosing $\nu > 1$. For $\nu = 1$, the model replicates dynamics where prey species do not cooperate. When $1 < \nu < 2$, partial cooperation enhances prey growth at a slightly reduced rate due to associated costs. However, for $\nu \geq 2$, the system loses its boundedness property, as the prey nullcline follows parabolic curve dynamics of a parabola with an upward opening. Now, we primarily vary the intensity of partial cooperation among prey species between $(1, 2)$ and the predators' attack rate while keeping it constant. Survival reliability is intrinsically linked to variations in environmental changes. To account for abrupt responses to these changes in the ecological setup, we consider how environmental fluctuations influence various factors (explained in detail in the introduction). Specifically, we identify the parameters ν (degree of partial cooperation) and ρ (predator consumption rate) as critical factors that vary under changing environmental conditions. Building on the approach by [1], we analyze the combined effects of environmental variation on ν and ρ. Under these considerations, our proposed model can be reformulated as follows:

$$\begin{aligned} \frac{dx}{dt} &= rx^{\nu} - ax^2 - dx - \frac{\rho xy^2}{1 + h\rho xy}, \\ \frac{dy}{dt} &= \frac{c\rho xy^2}{1 + h\rho xy} - my, \\ \frac{d\nu}{dt} &= \mu \qquad \textit{(environmental variation over cooperation of prey species),} \\ \frac{d\rho}{dt} &= \omega \qquad \textit{(environmental variation over predation rate).} \end{aligned} \tag{2.3}$$

Table 1. Definitions of parameters in model (2.3).

Symbol	Description
r	Birth rate of the prey species
ν	Degree of partial cooperation
a	Intra-specific competition of prey
d	Natural death rate of prey
ρ	Consumption rate of predator
h	Handling time of predator
c	Biomass conversion rate of predator
m	Natural death rate of predator

In the proposed model for a time-varying environment, we choose ρ as the second parameter to study the multi-parameter effects of environmental changes. The rationale for selecting ρ over ν is thoroughly

explored in the description of the two-parameter bifurcation in Section 6. We introduce a constant directional change in the parameters ν and ρ, expressed as $\nu = \nu_0 + \mu t$ and $\rho = \rho_0 + \omega t$, where ν_0 and ρ_0 are the initial values. The parameters representing environmental variability can take positive, negative, or zero values, indicating increasing, decreasing, or absent environmental changes, respectively. A positive sign represents growth in the biological parameters, while a negative sign signifies decline. Initially, we perform a bifurcation analysis of the model in the absence of environmental variation, followed by an exploration of species dynamics under environmental changes in both directions.

3. Equilibrium classification and its stability

Under a constant environment (i.e., when $\mu = 0$ and $\omega = 0$), we analyze the critical or equilibrium points of our system (2.3) as follows:

1) In the absence of the predator community, two scenarios are possible: (i) the extinction state, $E_0 = (0, 0)$, or (ii) the prey-only state, $E_{po} = (x_1, 0)$, where x_1 is/are the positive solution(s) of the equation:

$$r{x_1}^{\nu} - ax_1 - d = 0. \tag{3.1}$$

Theorem 1. *For $\nu \in (1, 2)$, the system has exactly two axial (predator-free nontrivial) equilibria.*

For the detailed proof, see the Appendix.

2) In the presence of the predator community under a constant environment (i.e., when $y \neq 0$), the system (2.3) admits a coexistence equilibrium point(s), $E_{ce} = (x_*, y_*)$, where:

$$y_* = \frac{m}{\rho x_*(c - mh)},$$

and x_* is the positive solution of the equation:

$${x_*}^{\nu+1} - ax_*^3 - dx_*^2 - D = 0 \tag{3.2}$$

with $D = \frac{m^2}{\rho c(c-mh)}$.

To examine the stability of these equilibrium points under a constant environmental setup, we first compute the Jacobian matrix of the system (2.3) at any equilibrium $E = (x, y)$:

$$J(E) = \begin{pmatrix} J_{11} & J_{12} \\ J_{21} & J_{22} \end{pmatrix},$$

where:

$$J_{11} = r\nu x^{\nu-1} - 2ax - d - \frac{\rho y^2}{(1 + h\rho xy)^2},$$

$$J_{12} = \frac{\rho xy}{1 + h\rho xy}\left[\frac{h\rho xy}{1 + h\rho xy} - 2\right],$$

$$J_{21} = \frac{c\rho y^2}{(1 + h\rho xy)^2},$$

$$J_{22} = \frac{c\rho xy}{(1 + h\rho xy)^2}(h\rho xy + 2) - m.$$

The stability of an equilibrium point is determined by the eigenvalues of this Jacobian matrix. If any eigenvalue has a positive real part, the equilibrium is unstable. Conversely, if both eigenvalues have negative real parts, the equilibrium is stable.

The sign changes of these eigenvalues are further explored in the bifurcation analysis presented in the next section, where the dependency of parameter values on the stability exchange phenomenon is discussed. Additionally, we numerically visualize the behavior of these equilibrium points through the basin of attraction (see Figure 1). This analysis is consistent with previous studies, such as those by [34, 35], which emphasize the role of parameter variations and functional responses in shaping predator-prey dynamics.

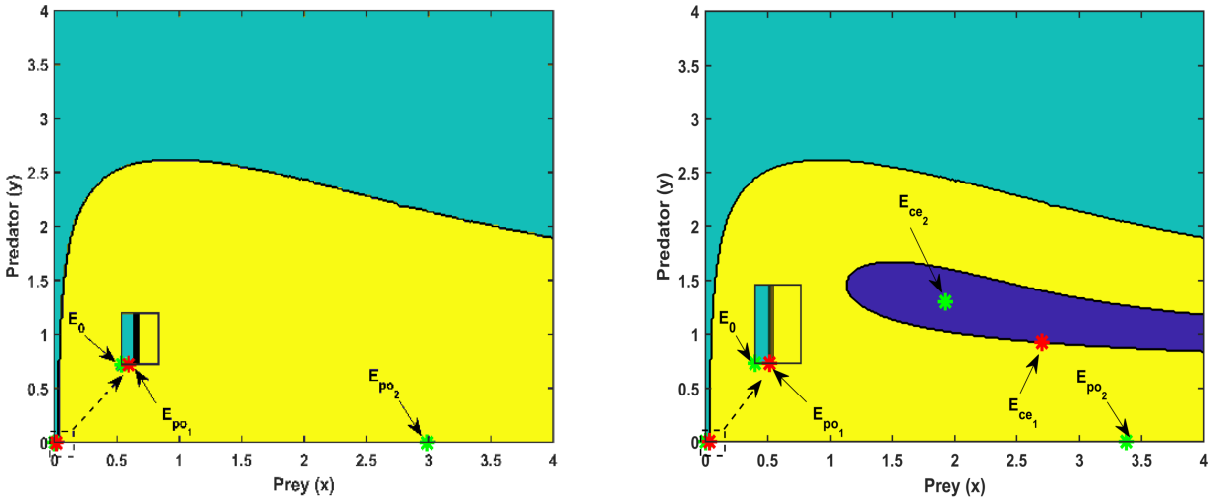

(a) (b)

Figure 1. The basins of attraction for the steady states E_0, E_{po_2}, and E_{ce_2} under a constant environment (i.e., when $\mu = 0$ and $\omega = 0$) are depicted in Figure 1. Figure 1(a) illustrates the basin structure at $\nu = 1.25$, where no predator survives in the community. Despite the absence of predators, the system exhibits two distinct basins of attraction: the sky-blue region corresponds to the extinction equilibrium E_0, while the yellow region corresponds to the predator-free stable equilibrium E_{po_2}. In contrast, Figure 1(b) shows the basin configuration at $\nu = 1.31$, where a new basin of attraction emerges due to the existence of the stable coexistence equilibrium E_{ce_2}, represented by the dark blue region. Equilibrium points are marked by asterisks ($*$), with green indicating stable equilibria and red indicating unstable ones, providing a comprehensive visualization of the system's dynamic behavior. To enhance clarity near the origin, where the basins appear more congested, both panels include a zoomed-in view to better capture the local dynamics.

In the constant environments, to verify the existence of positive solutions for Eqs (3.1) and (3.2) numerically, we set the parameter values as $r = 0.6$, $a = 0.2$, $d = 0.2$, $c = 0.45$, $m = 0.1$, $\rho = 0.1$, and $h = 0.5$. Throughout this paper, these parameter values are kept constant unless otherwise stated. Since Eqs (3.1) and (3.2) depend solely on the parameter ν, which is not fixed in our context, we first determine the valid range of ν where positive solutions exist. It is found that (in the detailed

analytical exploration found in [27]) positive solutions exist for ν in the range $1 \leq \nu \leq 2$. To study the classification of equilibrium points, we select two specific values of ν within this range and analyze the equilibrium points $E_{po} = (x_1, 0)$ and $E_{ce} = (x_*, y_*)$.

For $\nu = 1.25$, Eq (3.1) yields two positive solutions: $E_{po_1} = (0.013, 0)$ and $E_{po_2} = (2.9225, 0)$. Here, E_{po_1} is a saddle point with eigenvalues and eigenvectors -0.1, 0.48052 and $(0, 1)$, $(1, 0)$, respectively. On the other hand, E_{po_2} is stable, with eigenvalues and eigenvectors -0.38837, -0.1 and $(1, 0)$, $(-1.013 \times 10^{-6}, 1)$, respectively. In this scenario, the system dynamics show no coexisting equilibrium. Instead, there are two stable states: the extinction state $E_0 = (0, 0)$ and the prey-only state E_{po_2}. This is illustrated in the basin of attraction in Figure 1(a). Now, for $\nu = 1.31$, both Eqs (3.1) and (3.2) yield two positive solutions each. Specifically, the equilibrium points are $E_{po_1} = (0.03199, 0)$, $E_{po_2} = (3.3735, 0)$, $E_{ce_1} = (2.7028, 0.9250)$, and $E_{ce_2} = (1.9231, 1.3)$. Among these, two stable equilibrium states are observed: E_{po_2} and E_{ce_2}. The corresponding eigenvalues and eigenvectors for E_{po_2} are -0.40354, -0.1 and $(1, 0)$, $(-1.1114 \times 10^{-6}, 1)$, while those for E_{ce_2} are $-0.02562 + 0.11004i$, $-0.0256 - 0.11004i$ and $(0.93529, -0.25515 - 0.2452i)$, $(0.93529, -0.25515 + 0.2452i)$. The remaining equilibrium points are unstable and play a role in defining the boundaries of the basin of attraction (see Figure 1(b)).

4. Sensitivity analysis

To assess the influence of key parameters on predator abundance and infer implications for coexistence, we conducted a global sensitivity analysis by using Latin hypercube sampling (LHS) in combination with partial rank correlation coefficient (PRCC) analysis [36]. Although variance-based Global sensitivity and uncertainty analysis (GSUA) methods such as the Sobol indices, Morris screening, and FAST are increasingly used for capturing nonlinearities and high-order interactions [37], we chose PRCC for this study due to its balance of interpretability, computational efficiency, and wide acceptance in ecological modeling. In particular, PRCC allows us to rank monotonic parameter effects robustly and is well-suited for our goal of identifying the dominant drivers of predator persistence under dynamic environmental change. The structured design via Latin hypercube sampling ensures comprehensive coverage of the parameter space while maintaining computational tractability. This approach enables a comprehensive exploration of the parameter space, where each parameter was varied within 20% of its baseline value under a uniform distribution assumption. A total of 2000 simulations were performed, and predator abundance was treated as the response function for PRCC computation. The resulting PRCC values quantify both the strength and direction of each parameter's influence, as shown in Figure 2. The parameter with the strongest negative PRCC value is the *degree of cost-associated cooperation* (ν) in prey. Biologically, ν represents the intensity of cooperative behavior among prey species, such as coordinated foraging or group defense, that indirectly influences their reproductive success and survival under environmental stress. When ν increases, the system tends toward more intense cooperation, which in some ecological settings can become energetically costly or behaviorally restrictive. In such cases, while cooperation may confer local benefits to prey, its indirect effects may suppress population-level growth or flexibility, ultimately reducing food availability for predators and leading to lower predator biomass. This explains the observed negative correlation between ν and predator abundance.

Conversely, the predator *attack rate* (ρ) exhibits the strongest positive PRCC value. This is

expected, as a higher attack rate enhances the predator's ability to efficiently capture prey and sustain its biomass. The interplay between ν and ρ—as oppositely acting but environmentally sensitive parameters—captures a key eco-evolutionary feedback loop. Under deteriorating or heterogeneous environmental conditions, prey often resort to increased cooperative behaviors to manage risk, while predators respond by optimizing their foraging strategies. Thus, when prey species are forced to elevate cooperation due to habitat fragmentation or fear-driven stress, it may either reduce their reproductive output or amplify their density (depending on cost thresholds), both of which influence predator response. In turn, predators modulate their attack rate based on prey availability and the defense strategy, completing a natural adaptive cycle that governs coexistence. Other parameters, such as the intrinsic prey growth rate (r) and the cooperation amplification coefficient (a) do exhibit moderate positive PRCC values, indicating a potential influence on predator abundance. However, in this study, we intentionally held both (r) and (a) constant in order to isolate and explore the direct or indirect influence of the cost-associated cooperation strength (ν) on prey reproduction and abundance. Our aim was to understand how variations in ν, rather than changes in the intrinsic reproductive potential, impact overall system dynamics when the reproductive rate and cooperative amplification remain fixed. Although predator density is sensitive to (r) and (a), these parameters were excluded from the core analysis for this reason. The remaining parameters, including the death rate (d), conversion efficiency (c), and predator mortality (m), were also treated as constants to reflect their ecological stability over the relevant time scales.

Their relatively low PRCC values further support this decision, and their effects are consistent with known ecological roles, though not central to the specific feedback mechanisms we investigated.

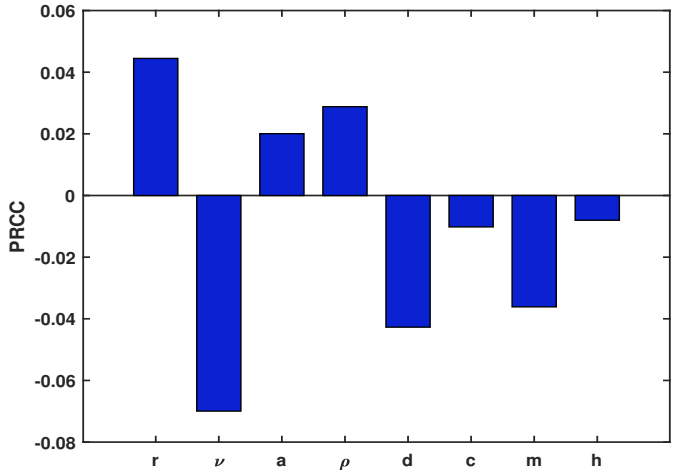

Figure 2. PRCC values of model parameters with respect to predator abundance. Positive values indicate parameters that enhance predator biomass, while negative values correspond to parameters that reduce it.

5. Exploring single parameter rate-dependent dynamics

Like general bifurcation analysis, which depends on the eigenvalues of the Jacobian matrix of the model (2.3), we first aim to explore the long-term dynamics of the community under a constant

environment. Specifically, we focus on the parameters ν (the rate of increase in prey abundance) and ρ (the predator's consumption rate). These parameters are crucial under environmental fluctuations. To understand their roles, we begin by examining the dynamical and ecological perspectives through single-parameter bifurcation analysis and then analyze their combined effects under environmental variations. All bifurcation diagrams presented in this paper were generated using MATCONT [38, 39] in MATLAB (version 2021a).

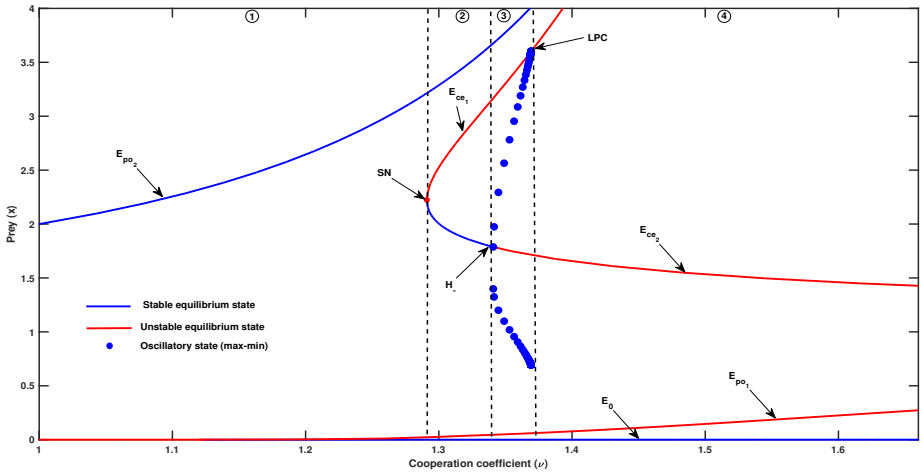

Figure 3. This figure illustrates the single-parameter bifurcation analysis of the system (2.3) under a constant environment with respect to the parameter ν. The blue line represents the stable states, while the red curve denotes the unstable states. The blue dot points indicate the maximum and minimum oscillation periods of the system for different values of ν, spanning from the H_- point to the homoclinic bifurcation point (LPC point). The regions separated by vertical dotted lines represent distinct dynamical and biological behaviors, which are explicitly discussed throughout this work.

In a constant environment, we first consider parameter ν (see Figure 3). When $\nu = 1.1$, the system exhibits three equilibrium states: the extinction state E_0 and two prey-only states, E_{po_1} and E_{po_2}. At this stage, the stable states E_0 and E_{po_2} are separated by the unstable prey-only state E_{po_1} (in Figure 3 at $\nu = 1.1$, the states E_0 and E_{po_1} are very close, although a small basin of attraction exists for the stable extinction state E_0, see Figure 1(a)). This means that, depending on the initial conditions, the system either converges to a high-density prey-only state or both species go extinct over time. As the rate ν decreases from 1.1 toward 1, the dynamics remain unchanged. However, increasing ν to 1.29 triggers a saddle-node bifurcation (SN), resulting in the birth of two new coexisting equilibrium states: one unstable (E_{ce_1}) and one stable (E_{ce_2}). Beyond this point, the system exhibits five equilibrium points: two unstable states (E_{po_1} and E_{ce_1}) and three stable ones (E_0, E_{po_2}, and E_{ce_2}). Up to $\nu = 2$, the stability of these points remains unchanged, except for E_{ce_2}. At $\nu = 1.345$, the stable coexisting state E_{ce_2} becomes unstable through a supercritical Hopf bifurcation (H_-), leading to stable periodic oscillations of both prey and predator populations over time—a phenomenon sometimes referred to as the "paradox of enrichment". As ν increases further, at $\nu = 1.75$, the oscillatory behavior disappears when the maximum amplitude of the oscillation touches the unstable state E_{ce_1} (see the *LPC* point

in Figure 3). All these bifurcation phenomena, including the creation of new states and transitions between stable and oscillatory dynamics, are depicted in Figure 3.

In this one-parameter analysis with respect to ν, the system's dynamics are divided into four distinct regions based on the long-term community behavior under a constant environment. These regions are illustrated in Figure 3 and form the foundation for further exploration. Below, we provide a detailed ecological interpretation of these regions, which will also inform subsequent bifurcation analyses concerning the parameter ρ.

(i). In region ①, the prey community dominates species survivability. The stable equilibrium point E_{po_2} has a larger basin of attraction than the extinction state E_0 (see Figure 1(a)). In this region, there is no coexisting equilibrium, and the predator population cannot persist over the long term. The outcome depends on the initial abundance of the community: if the prey population is insufficient, the entire community may go extinct. This highlights the critical role of a sufficiently high prey cooperation rate (ν) for species coexistence. A higher ν value promotes prey survival and increases the potential for partial cooperation within the prey community, which indirectly supports predator persistence.

(ii). In region ②, the system under a constant environment exhibits five equilibrium points, three of which are stable (E_0, E_{po_2}, and E_{ce_2}). The possible long-term outcomes are: (a) Extinction of both species (E_0), (b) Survival of the prey-only community (E_{po_2}), or (c) Coexistence of both species (E_{ce_2}). The community's trajectory depends on its initial conditions, reflecting the sensitivity of the ecosystem to its starting structure. This region demonstrates the transition from simple prey dominance to potential coexistence (see Figure 1(b)).

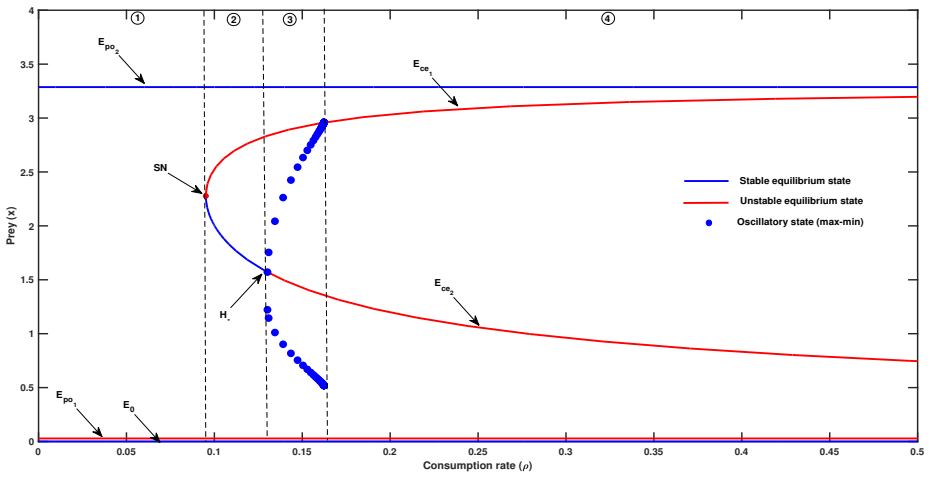

Figure 4. This figure presents the single-parameter bifurcation analysis of the system (2.3) in a constant environment, on the parameter ρ. The blue line indicates stable states, whereas the red curve highlights unstable states. The blue dot markers represent the maximum and minimum oscillation periods of the system for various values of ρ, extending from the H_- point to the *LPC* point.

(iii). The region ③ shares similarities with region ② but differs in a key aspect: the equilibrium point E_{ce_2} becomes unstable, and a stable limit cycle emerges. In this case, the long-term behavior is dynamic rather than static. Depending on the initial conditions: (a) both species may go extinct, (b)

only the prey population may survive, or (c) both species may coexist in oscillatory abundance over time (due to the stable limit cycle). The emergence of the limit cycle indicates periodic oscillations in species populations, highlighting the interplay between predator and prey in maintaining community dynamics under constant environmental conditions.

(iv). The region ④ resembles region ① in terms of ecological behavior, with the prey community dominating. However, unlike region ①, two additional unstable coexisting states (E_{ce_1} and E_{ce_2}) are present. Despite their presence, the community's behavior in this region remains similar to that in region ①: the predator population cannot persist over time, and the prey community determines the long-term dynamics.

We also explore the dynamics with respect to the predator consumption rate (ρ) at $\nu = 1.3$, as all possible dynamical outcomes (extinction, prey-only survival, and coexistence) occur in region ② for this parameter combination. Interestingly, the ecological behavior observed for varying ρ closely mirrors the dynamics described above for ν. Therefore, to avoid redundancy, we provide only the bifurcation diagram for ρ in Figure 4.

5.1. Effects of environmental variability

In recent years, the dynamics of ecological systems have increasingly been influenced by transient states—temporary phases in which communities exhibit unstable or intermediate behaviors. These transient states, driven by various biological and environmental factors, often lead to regime shifts, either reversible or irreversible, or critical transitions in community structure [40, 41]. Understanding these transient dynamics is essential for predicting long-term ecological outcomes and informing conservation strategies.

In this section, we investigate the transient dynamics of our model (2.3), focusing on rate-dependent variations of the system parameters ν (degree of partial cooperation in the prey species) and ρ (predator consumption rate). We also compare these findings with those observed under constant environmental conditions to highlight the impact of environmental fluctuations. Although the system becomes non-autonomous under time-varying parameters, we retain the equilibrium branches derived from the autonomous case as reference structures. These serve to interpret whether the evolving trajectory follows, departs from, or tips near the quasi-static equilibria and bifurcation points.

First, we examine the scenario where environmental fluctuations affect only the growth rate of the prey community ($\mu \neq 0, \omega = 0$). Under this condition, system (2.3) does not exhibit consistent solutions as in the constant environment case. As a result, the stability phenomena described earlier cannot be directly applied over a longer timescale. We simulate the system under these fluctuating conditions and plot the time series of prey population dynamics overlaid on the bifurcation diagram (Figure 3). Given that $\nu(t) = \nu_0 + \mu t$, each point in time corresponds to a specific value of the parameter ν. The magenta, black, and green curves in the plot represent the time-varying parameter ν on the horizontal axis, with the corresponding prey density measured on the vertical axis at each time point.

A key observation is the delayed response of the prey population compared to the constant environment scenario. When the time series crosses the bifurcation threshold, the system does not immediately settle into a stable state. Instead, it takes time—depending on the rate of environmental change (μ)—to reach the eventual stable state. This delay in response is often termed a "delayed response". During this transient phase, the community may temporarily reside in unstable states.

More specifically, it may "track" the unstable state of the corresponding constant environment setup. This phenomenon, termed "tracking unstable states" in previous studies [1, 42], highlights the system's tendency to follow unstable trajectories before converging to a stable equilibrium or periodic behavior.

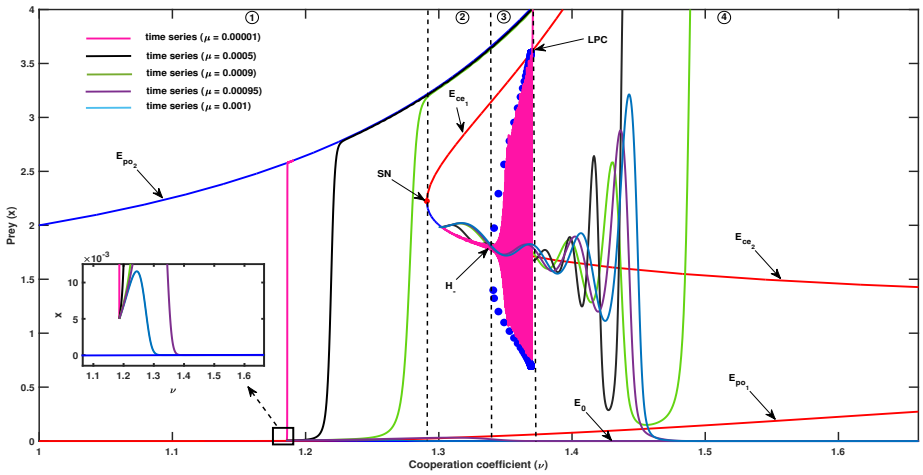

Figure 5. Rate-dependent dynamics in the model (2.3) under increasing environmental rate ($\mu > 0$) and $\omega = 0$: As the parameter ν increases over time at rates $\mu = 0.00001$ (magenta curve), $\mu = 0.0005$ (black curve), and $\mu = 0.0009$ (green curve), the model exhibits tracking of unstable states for a certain period. As ν continues to increase (for $\mu = 0.00095$ and $\mu = 0.001$, see the zoomed view on the left side of the figure), the rate-dependent time series ultimately converges to the extinction state E_0 under both scenarios: when the initial community density starts from region ① and region ②. The parameter values are set as follows: $r = 0.6$, $a = 0.2$, $d = 0.2$, $c = 0.45$, $m = 0.1$, $\rho = 0.1$, and $h = 0.5$.

Understanding this transient tracking behavior is crucial as it provides insights into how ecological communities respond to gradual environmental changes. It underscores the importance of accounting for transient dynamics in predicting ecosystem responses and managing biodiversity under fluctuating environmental conditions. As we divide the total parameter space ν into four regions, we begin by exploring the environmental effects in the first region. We initialize the system with low-density values for both prey and predator populations and analyze the time series dynamics starting at $\nu = 1.185$. For a very low rate of environmental fluctuation ($\mu = 0.00001$), the community growth does not exhibit any significant deviations (magenta curve in region ①, see Figure 5). This stability is attributed to the strong basin stability of the prey-only equilibrium state, E_{po_2} (see Figure 1(a)). In this case, the community directly tracks the stable prey-only state without any transient behavior, and the response time remains consistent over the simulation period.

5.1.1. Effects of positive environmental changes on the prey species

When the environmental rate changes increase slightly ($\mu = 0.0005$, the black curve in region ①, Figure 5), the dynamics differ from the previous case. Here, the time series temporarily tracks the unstable state, E_{po_1}, before settling at the stable prey-only state, E_{po_2}. This transient behavior emerges

despite the same initial conditions, suggesting that even a small increase in environmental variability can introduce transient states. If the environment becomes less favorable for prey, the community may experience a temporary collapse before stabilizing, with the dynamics accelerating compared to the lower fluctuation rate case. To further analyze the effect of increasing μ, we simulate the system for $\mu = 0.0009$ (green curve in Figure 5 in region ①). In this scenario, the time series tracks the unstable state E_{po_1} for a longer duration compared to the $\mu = 0.0005$ case. Moreover, the trajectory approaches the saddle-node (SN) bifurcation point before ultimately converging to the stable state E_{po_2}. Interestingly, as μ increases further, the community fails to survive. Simulations with higher μ values (also plotted in Figure 5) reveal that elevated rates of environmental fluctuation drive the prey population to extinction, leading to the collapse of the entire community.

5.1.2. Effects of positive environmental changes on coexisting states

In the preceding section, we analyzed the impact of environmental changes on the dynamics between the extinction state (E_0) and prey-only states (E_{po_1}, E_{po_2}). Notably, these fluctuations did not significantly affect the coexisting states (E_{ce_1}, E_{ce_2}), as the initial conditions were set near the lower community structure. To investigate further, we initialized the system closer to the SN bifurcation point by selecting initial conditions near the coexisting state E_{ce_2} at $\nu = 1.30$.

At very low rates of environmental variation ($\mu = 0.00001$), the dynamics of the coexisting community closely resemble those observed under constant environmental conditions. Depending on the time delay in species' responses, the system may exhibit stable coexistence with sufficient population densities, periodic oscillations, or transitions to prey-only survival scenarios. Thus, when the environmental fluctuation of the parameter ν remains minimal, the community can sustain itself in a healthy and balanced state. However, if such low-level variation persists over an extended period, the predator population may eventually go extinct. This extinction is primarily driven by the cooperative behavior of the prey species, which thrive under these mildly varying environmental conditions, ultimately undermining predator survival. This phenomenon is illustrated by the magenta trajectory in Figure 5, which begins near the saddle-node (SN) point in region ②.

However, at higher values of μ (e.g., $\mu = 0.0005, 0.0009$), the system increasingly tracks unstable states before transitioning to stable states. This tracking of unstable equilibria enhances the survivability of transient states and alters the long-term dynamics of the community. For $\mu = 0.001$, the transient behavior persists longer than for $\mu = 0.00095$ (see the corresponding time series curves for regions ② and ③ in Figure 5). In conclusion, increased rates of environmental variability (μ) can significantly influence community dynamics, particularly in triggering transient states. While constant environments fail to reveal such dynamics, the introduction of environmental fluctuations uncovers unstable state-tracking phenomena and enhances transient state survivability. These findings suggest that even moderate environmental variability can critically impact species persistence and community stability, offering valuable insights into ecological resilience under changing environments.

5.1.3. Impact of negative environmental changes on community dynamics

The effect of environmental changes does not always lead to community growth or stability; in some cases, a stable community structure may collapse, or predator survivability may deviate from healthy ecosystem dynamics.

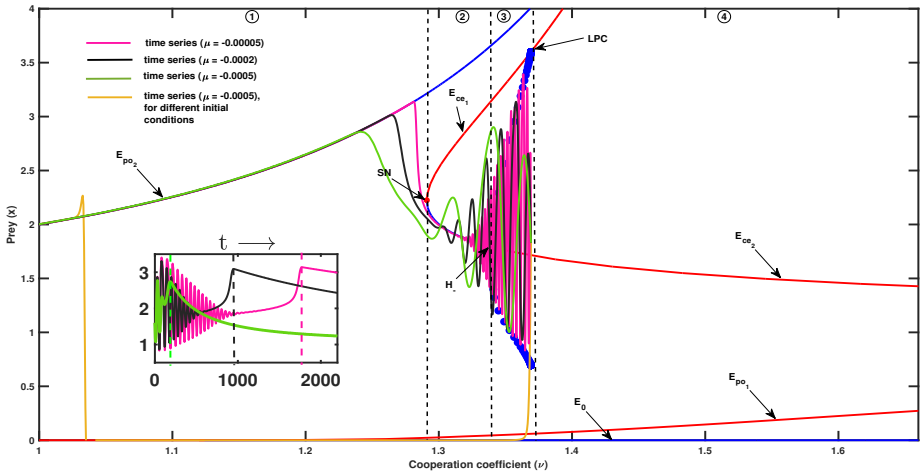

Figure 6. Rate-dependent dynamics in model (2.3) under $\omega = 0$ with decreasing environmental rate ($\mu < 0$): As the parameter ν decreases over time at rates $\mu = 0.00005$ (magenta curve), $\mu = 0.0002$ (black curve), and $\mu = 0.0005$ (green curve), the model exhibits tracking of unstable states for a certain period. The community dynamics demonstrate sensitivity to decreasing environmental rates, where the system temporarily follows unstable trajectories before transitioning to more stable configurations or extinction. The initial community density is set at the *LP* point within region ② (taken from under the constant environment setup). The parameter values remain consistent with those used in the positive environmental rate scenario, namely: $r = 0.6$, $a = 0.2$, $d = 0.2$, $c = 0.45$, $m = 0.1$, $\rho = 0.1$, and $h = 0.5$. These findings highlight the system's dynamic response to environmental decay, offering insights into resilience and tipping points within ecological systems. The subplot in the bottom left corner of this figure shows the time series of prey pollution for the same values of μ, with the dashed line indicating the corresponding critical transition time.

Therefore, exploring the influence of negative environmental rates on community dynamics becomes essential alongside positive fluctuations. This subsection investigates the impact of decaying environmental rates ($\mu < 0$) on species interactions and community structure. As with the positive rates of μ, we do not examine scenarios where the community starts from low-density initial conditions. Instead, we focus on coexisting states characterized by higher density values for both prey and predator populations. For this reason, we set the initial condition near a healthy population structure at $\nu = 1.36$. Under constant environmental conditions at this parameter value, the community exhibits periodic coexistence.

Starting with a low negative rate of environmental change ($\mu = -0.0005$), we run the system simulation (magenta curve starting from region ③ in Figure 6). The community does not significantly deviate from the dynamics observed in the constant environment scenario. Species densities continue to exhibit oscillatory behavior during the initial phase. However, near the SN bifurcation point, the time series shows minor deviations compared to the constant environment. Notably, no transient states or unstable state-tracking phenomena are observed at this low negative rate of environmental change of μ. As we increase the negative rate of environmental change to $\mu = -0.0002$ (black curve in Figure 6), noticeable deviations emerge. Although no unstable states are present, the community

maintains its oscillatory behavior. This contrasts with the constant environment case, where a supercritical Hopf bifurcation stabilizes the coexisting state. Over time, the deviation becomes more pronounced, and the system eventually tracks the stable prey-only state, E_{po_2}. For a higher negative rate of $\mu = -0.0005$ (green curve in Figure 6), transient phenomena persist for a longer duration compared to lower values of μ. The time series eventually tracks the prey-only state E_{po_2}, but the transient phase is extended.

Interestingly, while keeping the same initial conditions, the system maintains its coexistence behavior under these negative rates. However, changing the initial values dramatically alters the dynamics. With different starting conditions, negative environmental fluctuations can directly collapse the community, leading it to follow the extinction state (see yellow curve in Figure 6). Over an extended period, as basin stability diminishes, the system may suddenly transition to the prey-only state, particularly at low values of ν (e.g., $\nu = 1.035$).

Our findings reveal that negative environmental fluctuations can increase the duration of coexistence in a transient phase or drive the predator community to extinction, depending on the initial abundance of the community. These results highlight the complex and often unpredictable effects of environmental decay rates on community stability, emphasizing the need to consider both positive and negative environmental variations when analyzing long-term ecological dynamics.

5.2. *Effects of environmental fluctuations on the consumption rate of predators*

For the consumption rate (ρ) of the predator community, we also explore the environmental variation under both increasing rate and decreasing ω (when the intensity of prey cooperation is constant, i.e., $\mu = 0$ and $\omega \neq 0$). The tracking phenomenon is not different as compared to the exploration of the parameter ν. Therefore, we have not replicated the same things here, although in Figure 7, we briefly described the environment fluctuation results.

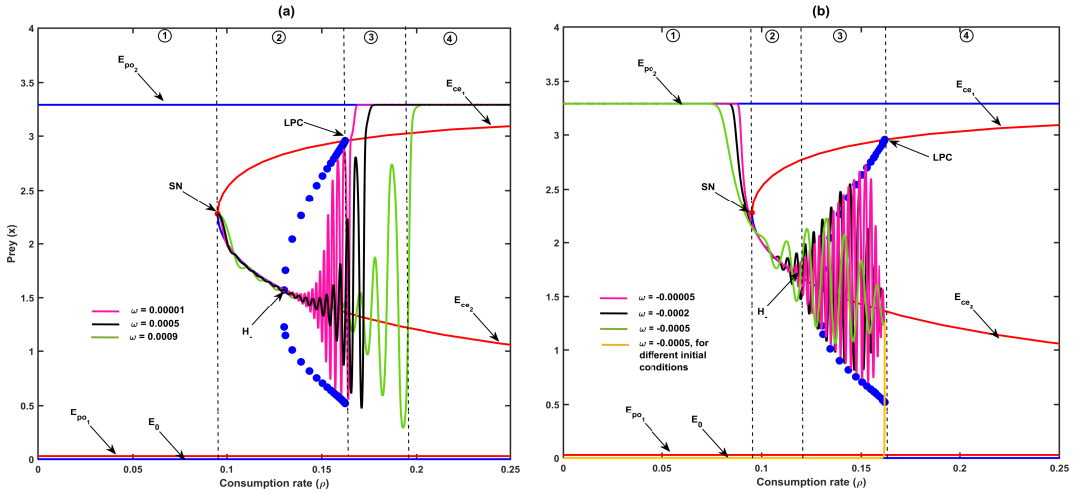

Figure 7. Rate-dependent dynamics in model (2.3) under $\mu = 0$ for both increasing ($\omega > 0$) and decreasing ($\omega < 0$) environmental rates: Figure 7(a) illustrates the system's response to positive changes in ω, while Figure 7(b) depicts the dynamics under negative rates of ω. The transient dynamics observed in both scenarios remain consistent with the outcomes obtained when starting from the same initial conditions near the *LP* point.

5.3. *Basin stability*

Our exploration is of the rate-dependent environment, i.e., the tracking phenomenon of our considered system (2.3) mainly on the bistable or tri-stable regions ②, ③, and ④, respectively, for both the positive and negative values of μ as well as ω. All the tracking phenomena or persistence of the transient state are dependent on the initial conditions. Then one question in our mind is that the representation of these outcomes may not be unique from the ecosystem perspective. We answer this question through basin stability from both constant and variable environments for each case as follows:

We choose the tri-stable region from our analysis, focusing on three specific parameter configurations to illustrate the stability dynamics: (1) For $\nu = 1.3$, $\rho = 0.1$, three stable steady states exist: the extinction state E_0, the prey-only state E_{po_2}, and the predator-prey coexistence state E_{ce_2}. (2) For $\nu = 1.36$, $\rho = 0.1$, three stable states are observed: the extinction state E_0, the prey-only state E_{po_2}, and a stable oscillatory state around the unstable equilibrium E_{ce_2}. These dynamics can be visualized in regions ② and ③ of Figures 3, 5 and 6. (3) For $\nu = 1.3$, $\rho = 0.15$, three stable states include the extinction state E_0, the prey-only state E_{po_2}, and a stable oscillatory state around the unstable equilibrium, E_{ce_2}. These dynamics are represented in region ② of Figures 4 and 7.

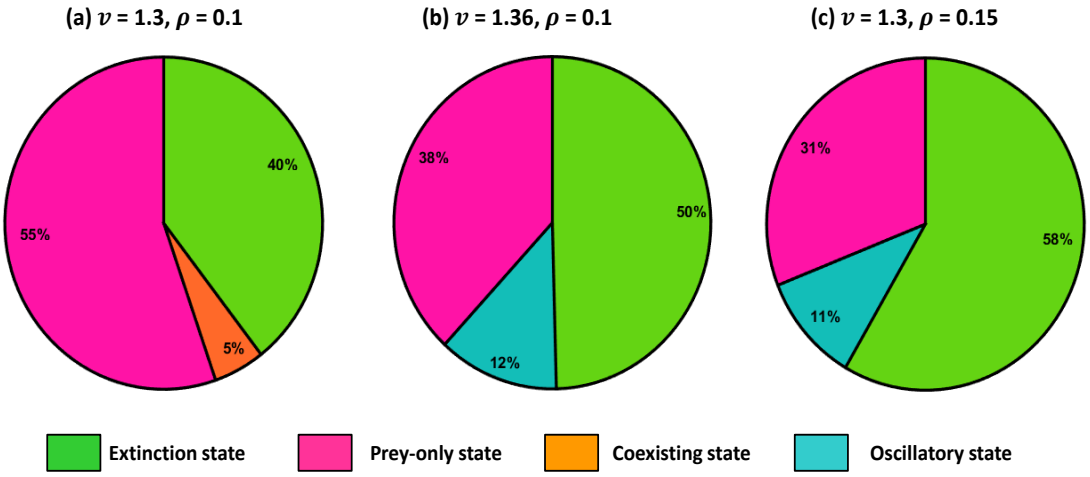

Figure 8. Basin stability: we randomly select 1000 initial points to evaluate the survival probabilities of particular steady states under a constant environmental rate (where both μ and ω are zero). In Figure 8(a), we focus on region ②, where all states E_0, E_{po_2}, and E_{ce_2} are stable under different initial conditions. However, in Figures 8(b),(c), we examine region ③, where the state E_{ce_2} becomes unstable, and stable oscillatory dynamics emerge around the unstable state E_{ce_2}.

To further explore these states, we select 1000 initial conditions (x_0, y_0). The initial conditions x_0 and y_0 were independently and uniformly sampled each from the interval $(0, 4)$ to ensure broad exploration of the phase space.

- First, when $\nu = 1.3$, $\rho = 0.1$, Figure 8(a) shows that approximately 55% of the trajectories converge to the prey-only state E_0, 40% lead to extinction, and only 5% remain in the co-existence state.

- Second, for $\nu = 1.36$, $\rho = 0.1$, Figure 8(b) reveals that 36% of the trajectories go to the prey-only state E_0, 51% lead to extinction, and 12% exhibit oscillatory behavior.
- Third, in the case of $\nu = 1.3$, $\rho = 0.15$, Figure 8(c) shows that 31% of the trajectories remain in the prey-only state E_{po}, 58% lead to extinction, and 11% exhibit oscillatory dynamics.

These results validate our analysis of transient dynamics and tracking phenomena, demonstrating that such dynamics can occur under various environmental changes. The interplay between initial conditions and environmental parameters highlights the complex behavior of ecological systems, providing critical insights into community resilience and stability.

6. Exploring bi-parameter influence over system dynamics

6.1. Bi-directional performance of our model under a constant environment

To explore more complex dynamics, we create two-parameter bifurcation diagrams concerning ν versus ρ. In Figure 9(a), the *LP* curve, Hopf curve, and *LPC* curve partition the bifurcation diagrams into four distinct regions. In Figure 9(a), with a moderate consumption rate of the predator ρ, gradually increasing the degree of partial cooperation leads the system into region ①, where a prey-only equilibrium state is observed.

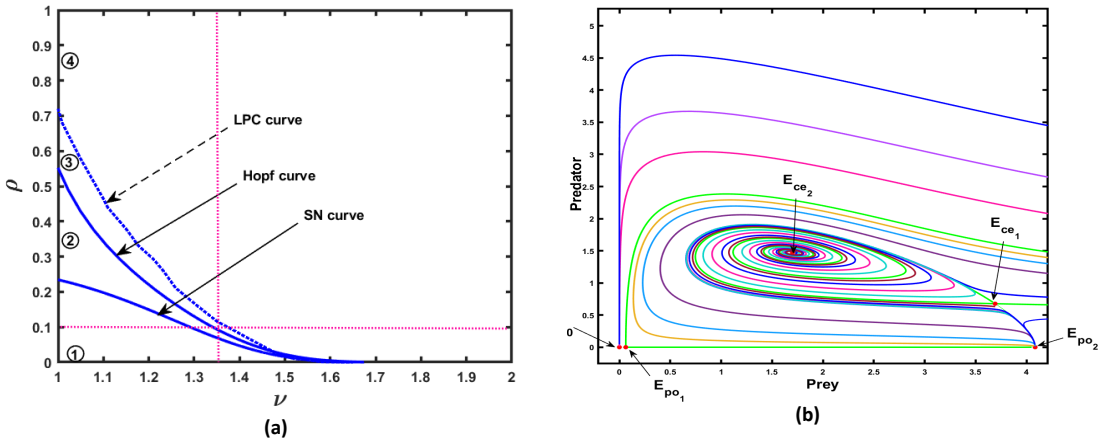

Figure 9. This figure illustrates the bidirectional parameter dependency on the community dynamics of our model (2.3) under a constant environment. Figure 9(a) depicts the dynamical findings, showing that parameter variation in the ν vs. ρ plane divides the space into four distinct regions. Figure 9(b) presents the phase portrait of system (2.3) at the intersection of the dotted line in Figure 9(a). The trajectories are color-coded to represent different initial conditions, with the green curve highlighting the basin separation boundary.

As the parameter ν is slowly increased, the system crosses the *LP* curve and transitions into region ②, where bi-stability emerges between the co-existing equilibrium state and the prey-only equilibrium state. After crossing the Hopf curve, the co-existing equilibrium becomes unstable, giving rise to limit cycle oscillations. Consequently, in region ③, we observe bi-stability between the

prey-only equilibrium and the limit cycle oscillations. At higher values of ν, the system crosses the *LPC* curve, causing the limit cycle oscillations to disappear through homoclinic bifurcation. This transition leads the system into region ④, where it becomes unstable due to heightened conflict between prey and predator. A phase portrait of the particular point in the ν vs. ρ plane is depicted in Figure 9(b).

In this study, the impact of environmental variation on the bi-parameter effect is primarily examined to capture changes in the sustainability period of species coexistence within the ecosystem. Through two-parameter variation analysis, we forecast the coexistence of asymptotic stable or oscillatory stable regions. By comparing two bi-parameter planes, we find that the ν vs. ρ plane offers more suitable parameter pairs than others. Therefore, in the bi-parameter study with time-varying environmental parameters, we proceed by focusing on the selection of ρ in conjunction with ν.

6.2. Environmental effect on a bi-parameter scenario and tracing ghost attractors

The results discussed above align with the existing concepts of the "tracking unstable state" phenomenon [1], demonstrating how the rate of environmental changes and initial conditions can shape species' long-term dynamics and potentially mitigate extinction risks. However, these findings also introduce an ambiguous conclusion: in the presence of extinction states as stable steady states, and in the absence of any coexistence states within the region of study, species extinction becomes an inevitable outcome. In such cases, irrespective of the initial conditions or the rate at which environmental changes influence the ecosystem, coexistence cannot be retained for a long time period.

While this scenario holds true for some species, recent studies suggest that global climate change can impose adverse conditions that accelerate extinction. However, the overall narrative reveals a more nuanced perspective. Although prolonged global climate change indeed increases extinction risks, species can adopt strategies to enhance their chances of survival in the interim. For example, during adverse climatic conditions, both prey and predator species may experience a decrease in metabolic rates, resulting in a decline in their gut-brain axes efficiency [20]. This metabolic decay could hinder prey species from efficiently acquiring resources individually, prompting them to exhibit more herd behavior. Such grouping tendencies may, in turn, help predators locate prey more easily, enhancing predation success rates [17,26]. Conversely, reduced predator metabolism may increase handling time, thereby lowering predation pressure as a simultaneous environmental effect [19, 43]. Additionally, as global warming drives prey species to adopt new foraging times or territories to avoid resource scarcity, predators may respond by increasing predation rates or seeking alternative resources. These adaptive behaviors could restore ecosystem balance and improve sustainability prospects [26].

Inspired by these biological insights, we aim to capture the effects of global climate change-induced prey grouping or herding behavior (modeled through the parameter ν) alongside simultaneous variations in predation rates (modeled through the parameter ρ). To maintain the biological rationality of this interaction, we alternate the signs of μ and ω in our model for each scenario, reflecting the dynamic interplay between environmental factors and species adaptation.

In Figure 10, we divide the entire range of the parameter ν (spanning $(1, 2)$) into three overlapping clusters. This fragmentation is necessary because, at different population densities and under varying rates of environmental influence on ν (denoted by μ), different rates of variation in predation rate ρ (denoted by ω) are required to delay extinction. Accordingly, we analyze (2.3) under the condition that both $\mu \neq 0$ and $\omega \neq 0$. Since both ν and ρ vary over time, the trajectory cannot wholly track any

one-parameter bifurcation state. Therefore, plotting time-series trajectories over a single-parameter bifurcation diagram would be impractical. However, fragmenting the domain of ν improves visualization and provides a rough estimate of the ultimate steady state that the trajectory may approach. The primary objective here is to enhance the sustainability of coexistence within the entire range of ν.

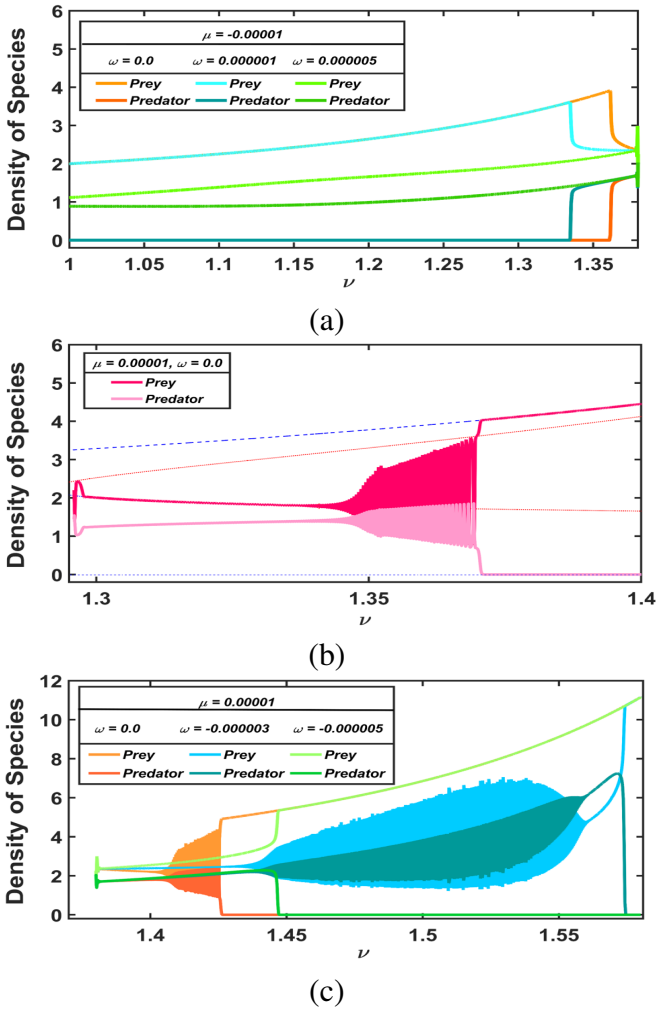

Figure 10. Rate-induced bi-parameter effect on species abundance: This figure illustrates the effects of environmental variation by dividing the entire range of ν into three critical segments. The middle panel (Figure 10(b)) captures species abundance when the environmental variation affects only the cooperation strength (with $\omega = 0$). In contrast, Figure 10(a) represents population dynamics within the range of $\nu \in (1, 1.38)$, and Figure 10(c) shows dynamics within the range of $\nu \in (1.38, 2)$, both considering variable environment-induced adaptive changes in the predation rate. In comparison to Figure 10(b), where predators remain unaffected by the environmental fluctuation rate (i.e., $\omega = 0$), the scenarios in Figure 10(a),(c) demonstrate a significant improvement in predator-prey survival when predators adapt their own predation strategies to environmental changes (i.e., $\omega \neq 0$). This adaptation leads to a notable increase in survival chances for both species, highlighting the importance of adaptive responses to dynamic environmental changes.

The middle panel of Figure 10(b) illustrates that when the environmental effect is not considered for the predation rate (i.e., $\omega = 0$), and $\mu = 0.00001$, both species coexist up to approximately $\nu = 1.38$. Eventually, the system transitions to a predator-free equilibrium, sustaining this state until about the $t = 4550$ time point (as discussed previously). However, as ω increases, the survival time extends proportionally. At $\omega = 0.000003$, the species' trajectories exhibit new dynamics, unobservable and unpredictable via one-dimensional or two-dimensional bifurcation analyses. Specifically, the trajectories (both prey and predator) initially converge toward a stable state up to around $t = 5000$. Subsequently, with increasing oscillations, they appear to cross a super-critical Hopf bifurcation point, following an oscillatory path up to approximately $t = 18{,}000$. At this stage, the trajectory mimics crossing an invisible sub-critical Hopf bifurcation, transitioning to a stable steady state. Near the $t = 19{,}200$ time point, the trajectories leave the stable coexistence state, heading toward the predator-free equilibrium and eventually merging into it.

These dynamics reveal how incorporating environmental effects across multiple parameters can significantly enhance species survivability. They also hint at the possible existence of "ghost attractors" in time-varying systems. Interestingly, further increases in ω begin to reduce species' chances of survival once more. To explore the backward dynamics depicted in Figure 10, we set $\mu = -0.00001$ and analyze three scenarios with $\omega = 0.0$, $\omega = 0.000001$, and $\omega = 0.000005$. In the first two cases, changes in ω have negligible effects. However, in the third case, with $\omega = 0.000005$, both species revive into the system and persist throughout the backward domain of ν (i.e., when $\nu \in (1, 1.37)$).

Bi-parameter changes indicate that suitable variations significantly enhance species survivability. However, the dependence of dynamics on initial parameter values remains ambiguous regarding robustness. While previous simulations focused on species persistence, we ask: What happens if a random initial condition is chosen from the basin space? The next subsection addresses this for both constant and variable environments.

6.3. Basin stability when both parameters change under environmental variation

We investigate the impact of environmental changes driven by both positive rates, μ and ω, on community dynamics, a concept that remains relatively unexplored. Following a similar setup to the constant environment scenario, we randomly select 1000 initial conditions (x_0, y_0) from the interval $(0, 4)$. In this rate-induced environment, no steady state exists, meaning the system continuously tracks different states depending on time. To analyze the time-dependent behavior, we examine the survival probabilities of the community over a broad time range as depicted in Figure 11.

First, we examine case (1), where $\nu = 1.3$ and $\rho = 0.1$ under a variable environment (see Figure 11). At early time points $T = 200$, $T = 500$, and $T = 2000$, the probability of coexistence remains relatively stable at around 7%, closely resembling the constant environment scenario. However, a notable trend emerges: the probability of transitioning to the prey-only state increases from 48% at $T = 200$ to 51% at $T = 2000$, indicating a gradual shift in system dynamics over time. This trend culminates at $T = 5000$, where the coexistence state disappears entirely. At this point, 57% of simulations converge to the prey-only state (E_{po_2}), while the remainder lead to the extinction state E_0. This sudden transition of the coexistence state between $T = 2000$ and $T = 5000$ is clearly visible in the pie diagrams (iii) and (iv) in Figure 11. To better understand this transition, we further simulate the system at intermediate time points $T = 3000$, $T = 3200$, and $T = 3500$ (see subfigures (a) to (c) in the inset of Figure 11). At $T = 3000$, the coexistence probability slightly declines to 5%; at $T = 3200$, it

drops further to 2%; and by $T = 3500$, the coexistence state vanishes entirely. These results indicate a smooth and continuous erosion of the coexistence basin, driven by persistent environmental variability. Overall, this analysis suggests that under this parameter configuration, gradual dual environmental changes erode the stability of the coexistence state. Over time, the system tends to favor either the prey-only state or total extinction, highlighting the vulnerability of community coexistence to sustained environmental fluctuations.

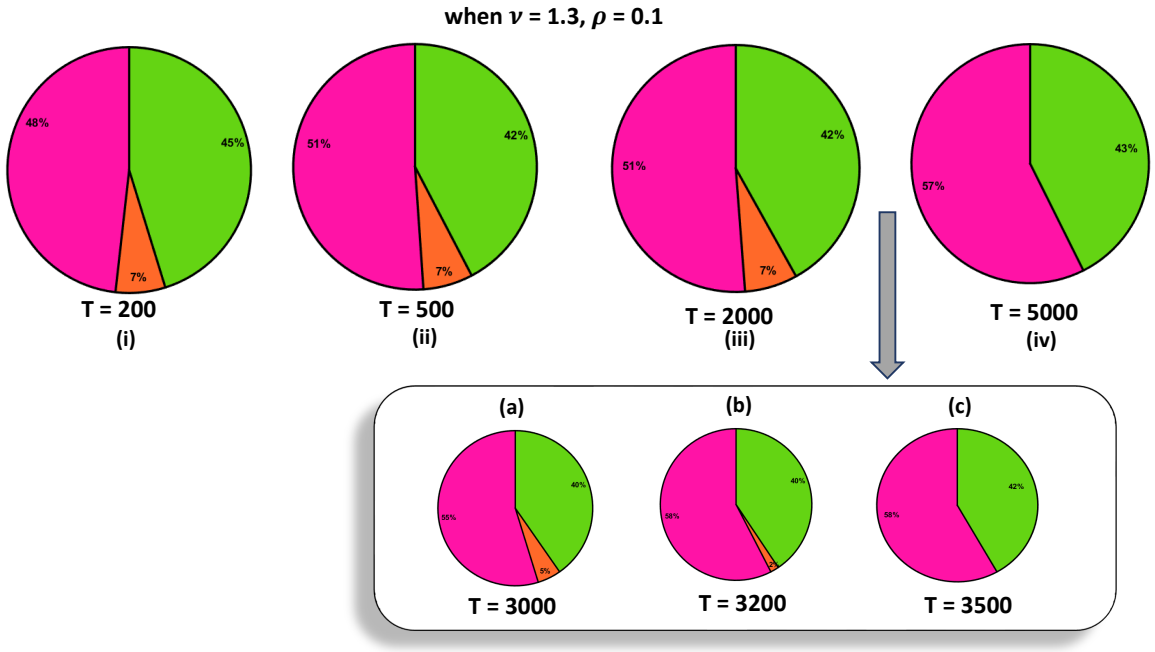

Figure 11. Panels (i–iv) illustrate the basin stability of system (2.3) at selected time points under varying environmental conditions, where $\mu \neq 0$ and $\omega \neq 0$. The specific time points are indicated below each corresponding pie diagram. The color scheme remains consistent with Figure 8, ensuring visual continuity and facilitating comparison across figures. For further details, refer to the main text.

We extended this analysis to two additional cases previously considered under constant environmental conditions. Interestingly, the results were contrasting and revealed new dynamics under dual environmental changes. Detailed descriptions and findings are presented in Figure 12(a),(b). In Figure 12(a), the upper four pie charts represent the same time scale as Figure 11. Here, the selected parameter values fall within region ③ under a constant environment. In this region, the coexisting equilibrium point E_{ce_2} is unstable, and a stable oscillatory dynamic exists around the unstable state E_{ce_2}. When both parameters ν and ρ vary over time due to environmental changes, the probability of tracking the unstable state in the oscillatory medium diminishes completely by the third time frame (see pie diagram (iii) in Figure 12(a)). Interestingly, the probability of prey species' survival continues to increase, similar to the case of Figure 11. For the third parameter setup, the first three pie diagrams are identical to those in Figure 11. However, as time progresses, the tracking probability for prey species decreases, while the extinction probability gradually rises. This suggests

that when environmental rates vary and the predator consumption rate becomes higher, the cooperative strategy of the prey plays a critical role in determining the community's fate. If the prey fails to adapt effectively, the entire community may face extinction under non-constant environmental changes. These results highlight the importance of dynamic adaptability and cooperation strategies in prey species for maintaining ecological stability in the face of varying environmental conditions.

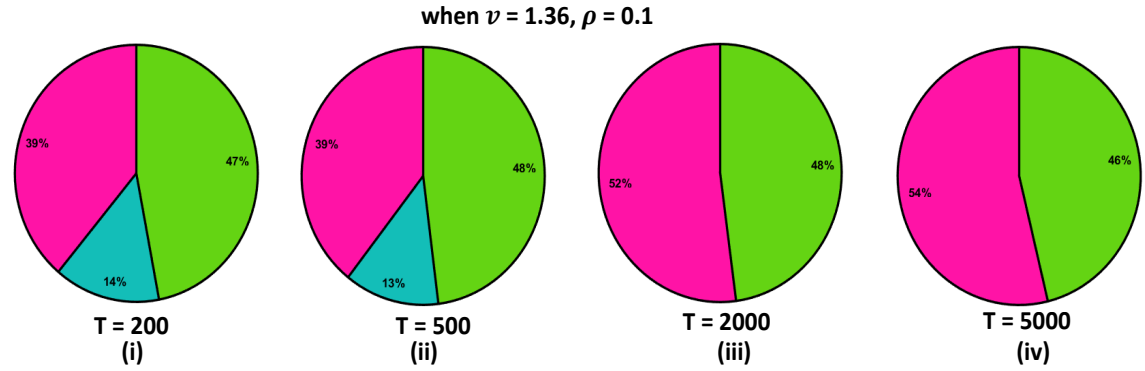

(a)

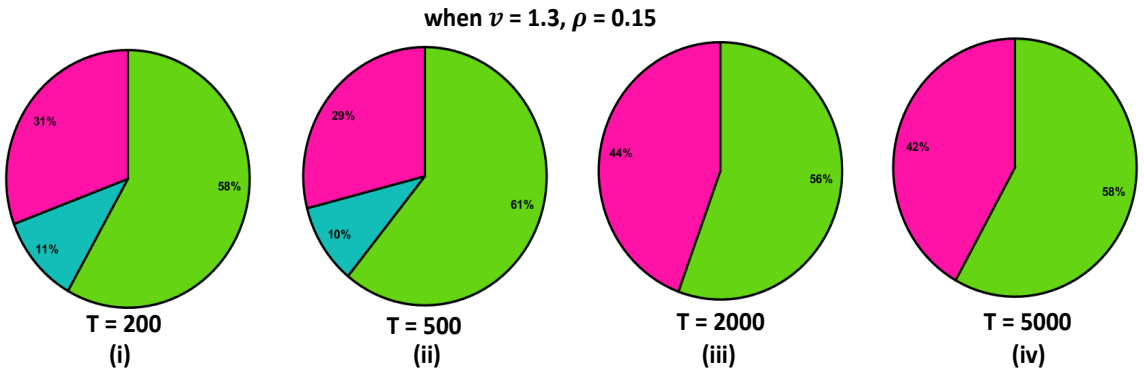

(b)

Figure 12. In this figure, we illustrate the time-dependent basin stability for the remaining two cases discussed earlier in the main text, and the color scheme used is consistent with that of Figure 8.

7. Discussion and conclusions

Environments continually evolve, reshaping species dynamics in complex and often unpredictable ways. Understanding species persistence and resilience requires examining both individual and community-level interactions alongside the impacts of environmental changes on biological traits [4, 28]. Fluctuating environments can push ecosystems toward new steady states or even extinction, depending on factors like initial population densities, species strategies, and environmental variation intensity. These abrupt transitions, known as regime shifts, are crucial in ecology as they often signal system collapse [44]. Environmental fluctuations frequently disrupt community stability, leading to transient states where species densities temporarily follow unstable trajectories [1, 42]. A significant focus of this study is rate-induced tipping (R-tipping), where rapid environmental changes

surpass a community's adaptive capacity, causing system instability [31]. Unlike bifurcation-induced tipping (B-tipping) or noise-induced tipping (N-tipping), R-tipping does not require critical thresholds or stochastic perturbations.

Most studies on regime shifts focus on abrupt changes, overlooking the rate of environmental variation [5, 28]. Our findings demonstrate that under identical resource conditions, species can reach different states solely due to environmental change rates. Rapid variation increases can trigger system collapse [16, 44]. Species typically track stable and unstable states sequentially, but as environmental variations intensify, tracking stable states weakens, accelerating transitions between ecological states [4]. Beyond the rate-dependent environmental effects, this study also investigates how cooperation-associated costs evolve in time-varying systems and their impact on long-term species dynamics. Before analyzing time-dependent models, it is crucial to first understand system behavior under constant environmental conditions. Our findings reveal that in the presence of cooperative interactions, both overcrowding and undercrowding can drive the ecosystem toward extinction [32]. Additionally, depending on the initial population density, species may settle into either a predator-free equilibrium or an extinction state [45], aligning with our model dynamics. It is well known that increasing cooperation intensity among prey enhances coexistence stability, facilitating predator reintroduction into the ecosystem. The dynamical results of our model not only capture these complex interactions but also reveal tristability, where the system progresses through oscillatory stable states before culminating in a homoclinic bifurcation. The presence of homoclinic and saddle-node bifurcations makes the system particularly intriguing under continuous environmental changes, as these transitions can induce tipping points or even ecosystem collapse [46]. Our findings suggest that both excessively low and high cooperation intensities can be detrimental to ecosystem stability. Moreover, an increasing degree of partial cooperation indicates that selective and heterogeneous cooperation strategies may impose greater costs than benefits, influencing species survival. Even in the absence of a stable coexistence state, the system retains multistability, with species fluctuating between predator-free equilibrium and total extinction.

The presence of a saddle-node bifurcation supports the theory of catastrophic collapse, as in a time-varying environment, a system moving in a particular direction may become unable to retrace its trajectory through the unstable state once it has passed a stable equilibrium. This forces the population into an irreversible transition to a new state [4, 5, 34]. Additionally, in the presence of multistability, the ultimate state of the system depends strongly on both the rate of environmental change and the initial conditions. Our results, particularly those examining decreasing cost-associated cooperation, capture similar biological dynamics, reinforcing the robustness of our numerical findings. Notably, such a dynamical outcome in a single-patch system remains an unexplored aspect of ecological modeling. This study also highlights that, under certain initial conditions, prey species that are initially prone to extinction at low cooperation intensity may experience a shift in survival probability as environmental variation intensifies. As cooperation declines more rapidly over time, predator populations, benefiting significantly from prey cooperation, are also severely affected. Since prey species incur substantial costs from cooperation, as observed in constant environments [27], both prey and predator densities decline sharply in response to increasing environmental variation. At an optimal rate of decline, when predator population density decreases more rapidly, prey species may gain an opportunity to recover within the ecosystem. More intriguingly, Figure (6) reveals a compelling dynamic where a trajectory initially near the homoclinic bifurcation first moves toward

extinction by passing through region ①, where typical prey trajectories with nonzero density tend to stabilize at the predator-free state. However, instead of following this expected path, the trajectory temporarily heads toward extinction before reversing and converging to a predator-free state. Such a rare yet possible phenomenon in a varying environment aligns with the well-known feed-forward mechanism [47]. This form of reversal dynamics remains relatively unexplored in studies on continuously changing environmental conditions, offering new insights into ecological resilience under dynamic constraints.

In realistic ecosystems, persistent stressors—such as global warming or elevated toxicity—can simultaneously weaken predator attack efficiency and reduce overall resource availability [20]. In response, prey may adopt intensified cooperative strategies like group foraging or sentinel behavior to enhance survival [19, 43], leading to cascading shifts across multiple traits. To capture this coupled response, we develop a novel eco-mathematical framework where two key parameters—the prey's cost-associated cooperation intensity (ν) and the predator's attack rate (ρ)—co-evolve under slow, irreversible environmental forcing. Unlike classical tipping studies focused on single-parameter changes, our dual-rate model reveals more nuanced, nonlinear transitions driven by predator-prey feedback. While constant-environment scenarios provide limited insight into long-term coexistence stability, our rate-induced basin stability analysis (applied here for the first time) shows how joint variation in ν and ρ governs the system's persistence. Notably, when both parameters vary in the same direction, the coexistence state gradually erodes, culminating in extinction (Figure 11); whereas reciprocal changes in ν and ρ can help sustain coexistence (Figure 10). Moreover, even under mild oscillations, a high predator attack rate combined with moderate prey cooperation sharply increases the likelihood of tipping toward extinction (Figure 12), underscoring the importance of adaptive dynamics in shaping ecosystem resilience. Variation in the same positive direction simultaneously intensifies both the predator attack rate and prey cooperative intensity, which, after crossing a certain threshold, incurs significant cooperation costs [27]. This dynamic places the persistence of prey—and consequently the predator—at risk. Maintaining this biological rationale, our results clearly show that while coexistence may persist temporarily, the long-term dynamics ultimately lead to total extinction beyond a critical tipping point.

In conclusion, the findings of this study illuminate how environmental fluctuations reshape species interactions, influencing persistence, stability, and extinction risks. This study highlights how rate-dependent environmental changes drive species toward different states, with rapid shifts potentially triggering collapse. Cooperative behaviors, while beneficial, can impose costs that vary with environmental intensity, leading to nontrivial survival dynamics. The presence of homoclinic and saddle-node bifurcations underscores tipping points and regime shifts affecting ecosystem stability. Understanding rate-induced tipping (R-tipping) is crucial for predicting species resilience. Exploration of environmental variation over a multi-parameter framework provides deeper ecological insights into the species' persistence mechanism. The findings pave the way for future research that integrates more complex ecological and environmental factors, ultimately contributing to more effective conservation strategies and ecosystem management.

This study analyzes prey-predator dynamics under environmental fluctuations, focusing on prey growth and predator consumption rates. Future research should incorporate stochastic variability to better understand noise-induced tipping (N-tipping) and species persistence [6]. Extending the model to multi-species systems and exploring adaptive behaviors like migration or cooperation can reveal

resilience mechanisms for both ecological and eco-epidemiological scenarios inspired by river networks under ecohydrological constraints [48]. Applying the framework to real ecosystems and climate projections may validate predictions and support conservation efforts. Though based on a simplified single-patch model, this work opens paths for empirical integration. A key next step is integrating our extinction-tipping framework with data-driven tools like convergent cross mapping (CCM) [49], which can detect causal links in nonlinear systems. Remote sensing data—especially long-term vegetation indices [50, 51]—offer promising avenues to validate model-predicted collapse patterns and cooperation-driven transitions, which also bridge theory with real-world complexity.

Use of AI tools declaration

The authors declare they have not used artificial intelligence (AI) tools in the creation of this article.

Acknowledgments

The authors sincerely thank the anonymous reviewers for their insightful and constructive feedback, which has greatly contributed to improving the clarity and overall quality of the manuscript. Suvranil Chowdhury, Sujit Halder (Grant Number: 4394/(CSIR-UGC NET JUNE 2018)), and Kaushik Kayal would like to acknowledge the Ministry of Social Justice & Empowerment, the University Grants Commission (UGC), and the Department of Science and Technology, Government of India, for their fellowship support, which made this research possible.

Conflict of interest

The authors declare there are no conflicts of interest.

References

1. R. Arumugam, F. Lutscher, F. Guichard, Tracking unstable states: Ecosystem dynamics in a changing world, *Oikos*, **130** (2021), 525–540. https://doi.org/10.1111/oik.08051
2. G. Keller, Impacts, volcanism and mass extinction: Random coincidence or cause and effect?, *Aust. J. Earth Sci.*, **52** (2005), 725–757. https://doi.org/10.1080/08120090500170393
3. L. W. Alvarez, W. Alvarez, F. Asaro, H. V. Michel, Extraterrestrial cause for the cretaceous-tertiary extinction, *Science*, **208** (1980), 1095–1108. https://doi.org/10.1126/science.208.4448.1095
4. M. Scheffer, S. R. Carpenter, Catastrophic regime shifts in ecosystems: Linking theory to observation, *Trends Ecol. Evol.*, **18** (2003), 648–656. https://doi.org/10.1016/j.tree.2003.09.002
5. M. Scheffer, S. R. Carpenter, T. M. Lenton, J. Bascompte, W. Brock, V. Dakos, et al., Anticipating critical transitions, *Science*, **338** (2012), 344–348. https://doi.org/10.1126/science.1225244
6. K. Siteur, M. B. Eppinga, A. Doelman, E. Siero, M. Rietkerk, Ecosystems off track: Rate-induced critical transitions in ecological models, *Oikos*, **125** (2016), 1689–1699. https://doi.org/10.1111/oik.03112

7. C. S. Holling, Resilience and stability of ecological systems, *Ann. Rew.*, **4** (1973), 1–23. https://doi.org/10.1146/annurev.es.04.110173.000245
8. C. Folke, S. R. Carpenter, B. Walker, M. Scheffer, T. Chapin, J. Rockström, Resilience thinking: Integrating resilience, adaptability and transformability, *Ecol. Soc.*, **15** (2010). https://doi.org/10.5751/ES-03610-150420
9. E. Zvereva, M. Kozlov, Consequences of simultaneous elevation of carbon dioxide and temperature for plant–herbivore interactions: A metaanalysis, *Global Change Biol.*, **12** (2006), 27–41. https://doi.org/10.1111/j.1365-2486.2005.01086.x
10. G. Woodward, N. Bonada, L. E. Brown, R. G. Death, I. Durance, C. Gray, et al., The effects of climatic fluctuations and extreme events on running water ecosystems, *Philos. Trans. R. Soc. B*, **371** (2016), 20150274. https://doi.org/10.1098/rstb.2015.0274
11. E. E. Cleland, I. Chuine, A. Menzel, H. A. Mooney, M. D. Schwartz, Shifting plant phenology in response to global change, *Trends Ecol. Evol.*, **22** (2007), 357–365. https://doi.org/10.1016/j.tree.2007.04.003
12. E. A. Ainsworth, S. P. Long, What have we learned from 15 years of free-air CO2 enrichment (FACE)? A meta-analytic review of the responses of photosynthesis, canopy properties and plant production to rising CO2, *New Phytol.*, **165** (2005), 351–372. https://doi.org/10.1111/j.1469-8137.2004.01224.x
13. C. L. Boggs, The fingerprints of global climate change on insect populations, *Curr. Opin. Insect Sci.*, **17** (2016), 69–73. https://doi.org/10.1016/j.cois.2016.07.004
14. D. Rubenstein, J. Kealey, Cooperation, conflict, and the evolution of complex animal societies, *Nat. Educ. Knowl.*, **3** (2010), 78.
15. M. Laparie, D. Renault, Physiological responses to temperature in Merizodus soledadinus (Col., Carabidae), a subpolar carabid beetle invading sub-Antarctic islands, *Polar Biol.*, **39** (2016), 35–45. https://doi.org/10.1007/s00300-014-1600-0
16. J. H. Brown, J. F. Gillooly, A. P. Allen, V. M. Savage, G. B. West, Toward a metabolic theory of ecology, *Ecology*, **85** (2004), 1771–1789. https://doi.org/10.1890/03-9000
17. L. I. Seifert, G. Weithoff, U. Gaedke, M. Vos, Warming-induced changes in predation, extinction and invasion in an ectotherm food web, *Oecologia*, **178** (2015), 485–496. https://doi.org/10.1007/s00442-014-3211-4
18. P. W. Sherman, Nepotism and the evolution of alarm calls: Alarm calls of Belding's ground squirrels warn relatives, and thus are expressions of nepotism, *Science*, **197** (1977), 1246–1253. https://doi.org/10.1126/science.197.4310.1246
19. F. Gao, F. Chen, F. Ge, Elevated CO2 lessens predation of Chrysopa sinica on Aphis gossypii, *Entomol. Exp. Appl.*, **135** (2010), 135–140. https://doi.org/10.1111/j.1570-7458.2010.00979.x
20. W. T. Hentley, A. J. Vanbergen, R. S. Hails, T. H. Jones, S. N. Johnson, Elevated atmospheric CO2 impairs aphid escape responses to predators and conspecific alarm signals, *J. Chem. Ecol.*, **40** (2014), 1110–1114. https://doi.org/10.1007/s10886-014-0506-1
21. B. T. Barton, Climate warming and predation risk during herbivore ontogeny, *Ecology*, **91** (2010), 2811–2818. https://doi.org/10.1890/09-2278.1

22. B. T. Barton, A. P. Beckerman, O. J. Schmitz, Climate warming strengthens indirect interactions in an old-field food web, *Ecology*, **90** (2009), 2346–2351. https://doi.org/10.1890/08-2254.1

23. A. Sentis, F. Ramon-Portugal, J. Brodeur, J. L. Hemptinne, The smell of change: Warming affects species interactions mediated by chemical information, *Global Change Biol.*, **21** (2015), 3586–3594. https://doi.org/10.1111/gcb.12932

24. T. Clutton-Brock, D. Gaynor, R. Kansky, A. MacColl, G. McIlrath, P. Chadwick, et al., Costs of cooperative behaviour in suricates (Suricata suricatta), *Proc. R. Soc. B*, **265** (1998), 185–190. https://doi.org/10.1098/rspb.1998.0281

25. A. Puentes, M. Torp, M. Weih, C. Björkman, Direct effects of elevated temperature on a tri-trophic system: Salix, leaf beetles and predatory bugs, *Arthropod-Plant Interact.*, **9** (2015), 567–575. https://doi.org/10.1007/s11829-015-9401-0

26. L. E. Culler, M. P. Ayres, R. A. Virginia, In a warmer Arctic, mosquitoes avoid increased mortality from predators by growing faster, *Proc. R. Soc. B*, **282** (2015), 20151549. https://doi.org/10.1098/rspb.2015.1549

27. S. Chowdhury, S. Sarkar, J. Chattopadhyay, Modeling cost-associated cooperation: A dilemma of species interaction unveiling new aspects of fear effect, preprint, arXiv:2501.16522.

28. M. Scheffer, S. Carpenter, J. A. Foley, C. Folke, B. Walker, Catastrophic shifts in ecosystems, *Nature*, **413** (2001), 591–596. https://doi.org/10.1038/35098000

29. R. Arumugam, F. Guichard, F. Lutscher, Persistence and extinction dynamics driven by the rate of environmental change in a predator-prey metacommunity, *Theor. Ecol.*, **13** (2020), 629–643. https://doi.org/10.1007/s12080-020-00473-8

30. P. J. Menck, J. Heitzig, N. Marwan, J. Kurths, How basin stability complements the linear-stability paradigm, *Nat. Phys.*, **9** (2013), 89–92. https://doi.org/10.1038/nphys2516

31. P. Ashwin, S. Wieczorek, R. Vitolo, P. Cox, Tipping points in open systems: Bifurcation, noise-induced and rate-dependent examples in the climate system, *Philos. Trans. R. Soc. A*, **370** (2012), 1166–1184. https://doi.org/10.1098/rsta.2011.0306

32. C. Cosner, D. L. DeAngelis, J. S. Ault, D. B. Olson, Effects of spatial grouping on the functional response of predators, *Theor. Popul. Biol.*, **56** (1999), 65–75. https://doi.org/10.1006/tpbi.1999.1414

33. B. L. Partridge, J. Johansson, J. Kalish, The structure of schools of giant bluefin tuna in Cape Cod Bay, *Environ. Biol. Fishes*, **9** (1983), 253–262. https://doi.org/10.1007/BF00692374

34. R. M. May, *Stability and Complexity in Model Ecosystems*, Princeton University Press, 2019.

35. C. S. Holling, The components of predation as revealed by a study of small-mammal predation of the European Pine Sawfly, *Can. Entomol.*, **91** (1959), 293–320. https://doi.org/10.4039/Ent91293-5

36. S. Marino, I. B. Hogue, C. J. Ray, D. E. Kirschner, A methodology for performing global uncertainty and sensitivity analysis in systems biology, *J. Theor. Biol.*, **254** (2008), 178–196. https://doi.org/10.1016/j.jtbi.2008.04.011

37. F. Pianosi, K. Beven, J. Freer, J. W. Hall, J. Rougier, D. B. Stephenson, et al., Sensitivity analysis of environmental models: A systematic review with practical workflow, *Environ. Modell. Software*, **79** (2016), 214–232. https://doi.org/10.1016/j.envsoft.2016.02.008

38. A. Dhooge, W. Govaerts, Y. A. Kuznetsov, MATCONT: A MATLAB package for numerical bifurcation analysis of ODEs, *ACM Trans. Math. Software*, **29** (2003), 141–164. https://doi.org/10.1145/779359.779362

39. A. Dhooge, W. Govaerts, Y. A. Kuznetsov, H. G. E. Meijer, B. Sautois, New features of the software MatCont for bifurcation analysis of dynamical systems, *Math. Comput. Modell. Dyn. Syst.*, **14** (2008), 147–175. https://doi.org/10.1080/13873950701742754

40. A. Hastings, K. C. Abbott, K. Cuddington, T. Francis, G. Gellner, Y. C. Lai, et al., Transient phenomena in ecology, *Science*, **361** (2018), eaat6412. https://doi.org/10.1126/science.aat6412

41. K. T. Frank, B. Petrie, J. A. Fisher, W. C. Leggett, Transient dynamics of an altered large marine ecosystem, *Nature*, **477** (2011), 86–89. https://doi.org/10.1038/nature10285

42. P. E. O'Keeffe, S. Wieczorek, Tipping phenomena and points of no return in ecosystems: Beyond classical bifurcations, *SIAM J. Appl. Dyn. Syst.*, **19** (2020), 2371–2402. https://doi.org/10.1137/19M1242884

43. A. N. Laws, Climate change effects on predator-prey interactions, *Curr. Opin. Insect Sci.*, **23** (2017), 28–34. https://doi.org/10.1016/j.cois.2017.06.010

44. G. Gundersen, E. Johannesen, H. Andreassen, R. Ims, Source-sink dynamics: How sinks affect demography of sources, *Ecol. Lett.*, **4** (2001), 14–21.

45. Y. A. Kuznetsov, *Elements of Applied Bifurcation Theory*, Springer, 1998.

46. O. J. Schmitz, B. T. Barton, Climate change effects on behavioral and physiological ecology of predator-prey interactions: Implications for conservation biological control, *Biol. Control*, **75** (2014), 87–96. https://doi.org/10.1016/j.biocontrol.2013.10.001

47. J. R. Bernhardt, M. I. O'Connor, J. M. Sunday, A. Gonzalez, Life in fluctuating environments, *Philos. Trans. R. Soc. B*, **375** (2020), 20190454. https://doi.org/10.1098/rstb.2019.0454

48. L. Carraro, F. Altermatt, A. Rinaldo, River networks as ecological corridors: A coherent ecohydrological perspective, *Adv. Water Resour.*, **113** (2018), 27–43. https://doi.org/10.1016/j.advwatres.2018.01.011

49. G. Sugihara, R. May, H. Ye, C. H. Hsieh, E. Deyle, M. Fogarty, et al., Detecting causality in complex ecosystems, *Science*, **338** (2012), 496–500. https://doi.org/10.1126/science.1227079

50. M. A. Campo-Bescós, R. Muñoz-Carpena, D. A. Kaplan, J. Southworth, L. Zhu, P. R. Waylen, Beyond precipitation: Physiographic gradients dictate the relative importance of environmental drivers on savanna vegetation, *PLOS ONE*, **8** (2013), e72348. https://doi.org/10.1371/journal.pone.0072348

51. M. A. Campo-Bescós, R. Muñoz-Carpena, J. Southworth, L. Zhu, P. R. Waylen, Combined spatial and temporal effects of environmental drivers on long-term NDVI dynamics in the African savanna, *Remote Sens.*, **5** (2013), 6513–6538. https://doi.org/10.3390/rs5126513

Appendix

Mathematical analysis

Persistence and boundedness

You should verify the boundedness and persistence results from [27], as the reduced dynamics in this study follow a similar structure.

Equilibrium points classification and their stability

Under a constant environment (i.e., when $\mu = 0$ and $\omega = 0$), we analyze the critical or equilibrium points of our system (2.3) as follows:

In the absence of the predator community, two scenarios are possible: (i) the extinction state, $E_0 = (0, 0)$, or (ii) the prey-only state, $E_{po} = (x_1, 0)$, where x_1 is/are the positive solution(s) of the equation:

$$r{x_1}^{\nu} - ax_1 - d = 0.$$

Condition for the existence of axial equilibria

Due to the complexity of the model, determining the exact form and locations of the axial equilibria is challenging. For $\nu = 1$, model (2.3) reduces to the classical competitive predator-prey system. We exclude this case and focus on the interval $\nu \in (1, 2)$, where the system has two axial equilibrium points: one to the left and one to the right of $(x_1^1, 0)$.

Theorem 2. *For $\nu \in (1, 2)$, the system has exactly two axial equilibria (predator-free equilibria).*

Step 1: Finding the number of axial equilibria

For $y = 0$, from the first equation of system (2.2), we get:

$$f(x_1) = r_0 x_1^{\nu-1} - ax_1 - d = 0. \tag{A.1}$$

The number of equilibria corresponds to the intersections of the prey nontrivial nullcline with the line $y = 0$. Let $\nu \in \mathbb{R}$ and $0 \leq \nu - 1 < 1$. We consider two cases.

Case 1: Rational $\nu \in \mathbb{Q}$

Let $\nu - 1 = \frac{\alpha'}{\beta'}$ with $\alpha', \beta' \in \mathbb{Z}, \beta' \neq 0$, and $\alpha' < \beta'$. After simplification, Eq (A.1) becomes:

$$f(w) = aw^{\beta'} - r_0 w^{\alpha'} + d = 0, \quad \text{where } w = x_1^{1/\beta'}. \tag{A.2}$$

By Descartes' rule of signs, the polynomial (A.2) has either two real positive roots or none. The function $f(x_1)$ is continuously differentiable for $x_1 > 0$, and we find:

$$f'(x_1) = r_0(\nu - 1)(\nu - 2)x_1^{\nu-3} < 0 \quad \text{for } x_1 \in (0, \infty),$$

indicating that $f(x_1)$ attains a maximum at $x_1 = x_1^1$. Since $f(0) < 0$ and $f(x_1^1) > 0$, the prey nullcline intersects the $y = 0$ line at exactly two distinct points: $(\alpha, 0)$ and $(\beta, 0)$, where $\alpha < x_1^1 < \beta$. Hence, the following conditions hold:

$$\alpha^{\nu-2} > \frac{a}{r_0(\nu - 1)} > \beta^{\nu-2}.$$

When $f(x_1^1) = 0$, the line $y = 0$ becomes tangent to the curve, resulting in a single axial equilibrium. This case is analyzed in the bifurcation section.

Case 2: Irrational $\nu \in \mathbb{R} \setminus \mathbb{Q}$

For irrational ν, there exist rational numbers m' and ν such that $m' < \nu < n'$. When $x_1 > 1$:

$$r_0 x_1^{m'} - a x_1 - d < r_0 x_1^{\nu} - a x_1 - d < r_0 x_1^{n'} - a x_1 - d, \tag{A.3}$$

and for $x_1 \leq 1$:

$$r_0 x_1^{m'}{}_1 - a x_1 - d \geq r_0 x_1^{\nu} - a x_1 - d \geq r_0 x_1^{n'} - a x_1 - d. \tag{A.4}$$

Thus, a curve with an irrational power lies between two curves with rational powers. As in Case 1, the curve intersects the $y = 0$ line at exactly two points. The conditions (A.3) and (A.4) derived for Case 1 also hold in Case 2, ensuring two axial equilibria for any real ν where $1 < \nu < 2$.

AIMS Press